Monitoring of a Historical Masonry Structure in Case of Induced Seismicity

Ihsan Engin Bal*[1], Dimitris Dais[1,2], Eleni Smyrou[1], Vasilis Sarhosis[2]

[1]Research Center for Built Environment NoorderRuimte, Hanze University of Applied Sciences, Zernikeplein 11, Groningen, The Netherlands

[2]School of Civil Engineering, University of Leeds, LS2 9JT, Leeds, UK

Abstract

In case of induced seismicity, expectations from a structural monitoring system are ~~also~~ different than in the case of natural seismicity. In this paper, monitoring results of a historical building in Groningen (Netherlands) in case of induced seismicity has been presented. Results of the monitoring, particularities of the monitoring in case of induced earthquakes, as well as the usefulness and need of various monitoring systems for similar cases are discussed. Weak soil properties dominate the structural response in the region, thus the ground water monitoring as well as the interaction of soil movements with the structural response have also be scrutinized. The proposed study could be effectively used to monitor historical structures subjected to induced seismicity and provide useful information to asset owners to classify the structural health condition of structures in their care.

It was shown that the in-plane cracks at the building would normally not be expected in this structure during small induced earthquakes happening in Groningen. One explanation provided here is that the soil parameters, such as shrinking of water-sensitive soil layers, in combination with small earthquakes, may cause settlements. The soil effects may superimpose with the earthquake effects eventually causing small cracks and damage.

*Corresponding Author: Ihsan Engin Bal, i.e.bal@pl.hanze.nl, +31 050 5952101

1. Introduction

Groningen is a gigantic gas field that has been exploited since 1963. However, an induced seismicity event in the field was first recorded in 1991 with local magnitude (ML) 2.4. In the subsequent years, there have been more than 1,300 registered small-magnitude earthquakes, the largest of which was ML 3.6 in 2012 (van Thienen-Visser and Breunese 2015). Groningen has been turned into the spearhead of the research related to induced seismicity in the recent years as it is the most intensely populated area in the world with many induced earthquakes. A list of recent research on the Groningen earthquakes can be found in (Smyrou and Bal 2019) as well as in (van Elk and Doornhof 2017).

Most of the buildings in the region are unreinforced masonry (Crowley et al. 2017). Local construction techniques, together with a number of other parameters, render the building stock seismically vulnerable even for these small magnitude earthquakes. For example, the structures built after the World War II consist of two-leaf cavity walls, an additional weakness to the inherent weaknesses of masonry. The extended damages of structures in recent years and the public outcry, and the motivation behind an immense research programme commissioned by the licensee company extracting the gas, NAM (Nederlandse Aardolie Maatschappij).

Considerable research work to assess the mechanical behaviour of typical masonry constructions as well as to evaluate their damage potential when exposed to induced seismicity has been carried out in parallel to extensive experimental studies (Graziotti et al. 2017; Graziotti, Penna, and Magenes 2019; Messali et al. 2018; Esposito et al. 2019; Sarhosis et al. 2019b; Sarhosis et al. 2019a). Moreover, there are more than 2,000 registered historical monuments in the Groningen region, the earthquake safety and structural integrity of which during these repeated small magnitude induced earthquakes is a major concern for the authorities, local communities and owners. The cultural heritage structures in the region consist of the traditional Dutch farmhouses inherited from generation to generation, churches together with surrounding premises belonging to them, public and administrative buildings of importance, residential houses, towers and noble houses (*"borg"* structures).

Despite the high concentration of historical buildings in the gas field, their seismic vulnerability and the past damages, there is solely one historical masonry building in the region where standard seismic Structural Health Monitoring (SHM) methods are applied. Though there are some sensors installed for different purposes in various ways (Bal 2018) in some other historical buildings in the region, interestingly enough no other heritage structure has a complete monitoring system, while at the same time there are accelerometer sensors in more than 400 houses, together with more than 50 strong ground motion stations of KNMI (The Royal Dutch Meteorological Institute) (KNMI 1993).

Historical masonry buildings are often complex structures in the sense of use of non-standardized materials and largely varying construction practises. This is reason why a case-specific SHM scheme ought to be developed to obtain a precise structural assessment. A SHM strategy should include long term plans, preferably a year and more if possible, so that changes in environmental conditions can be reflected in measurements. As an example, although slightly less than a yearlong monitoring was conducted, (Kita, Cavalagli, and Ubertini 2019) successfully investigated temperature effects on the static and dynamic response of an iconic Italian monumental palace. Data from crack and temperature measurements were combined with a continuous modal identification system and a calibrated numerical model for over a year course providing a better insight of the initial condition of the structure and enabling an accurate damage detection process. They have combined the crack amplitudes with temperature and the vibration results. Another example in environmental effects and the use of the SHM strategy in combination with those effects is the study by (Ramos et al. 2010) where they report

results from two complex historical structures consisted of continuous measurements of vibration temperature and relative air humidity. In their study, the dynamic characteristics of the structures are obtained by operational modal analysis (OMA) and subsequently statistical analysis are performed to evaluate the environmental effects on the dynamic response allowing the detection of damage at an early stage. (Ceravolo et al. 2017) show results from a long-term monitoring where 10-year monitoring results provided conclusions regarding a strengthening measure that took place in the past. The effect of the environmental changes on structural response, as well as the long-term monitoring in correspondence to determining the efficacy of structural strengthening, fall into the scope of this paper as explained later.

Given the necessity to preserve the authentic style of the monumental structures invasive test techniques are hardly allowed. When permission is granted by the preservation authorities, non-destructive testing techniques are implemented to contemplate the findings from SHM (L. M. S. Gonçalves, Rodrigues, and Gaspar 2017). Particularly, in case of a post-earthquake diagnosis the geometric survey and visual inspections are used in parallel with ambient vibration tests, sonic and flat-jack tests and the monitoring of vibration and temperature act as a seismic early warning system (Saisi and Gentile 2015; Rossi and Rossi 2015). Extensive structural monitoring networks have been deployed in regions with high seismic activity focusing on historical structures (Çaktı and Şafak 2019), while decisions for seismic retrofitting of historical structures are based on the monitoring data in an example by (Erdik 2018). It should also be stated that continuous measurements could provide valuable information for damage diagnosis and help to develop a smart maintenance plan as reported by (Cigada et al. 2017) and (Coïsson and Blasi 2015).

The aim of this paper is to present monitoring results of a historical building in Groningen (Netherlands) subjected to induced seismicity. Results of the monitoring, particularities of the monitoring in case of induced earthquakes, as well as the usefulness and need of various monitoring data for similar cases are discussed. Effect of the changes in the environmental conditions and its relevance to monitoring in case of induced seismicity are discussed

2. Induced earthquakes in Groningen

Groningen is the largest on-land gas field in the world and is being exploited since 1963, with gas initially in place (GIIP) of close to 3000 billion m^3 (bcm) (van Thienen-Visser and Breunese 2015). Almost 3 quarters of the gas has been extracted since then resulting in a maximum soil compaction of 30 cm in the heart of the gas field (NAM 2016). The compaction and the decrease of internal pressure in the reservoir inflicted earthquakes since early 90s. More than 1,300 earthquakes have been recorded in the region all attributed to the gas extraction activities since the region was totally silent in terms of prior seismic activity. The largest earthquake recorded so far was of ML 3.6 in 2012 with the largest horizontal Peak Ground Acceleration (PGA) of 0.08 g, and the largest ever horizontal PGA recorded as 0.11 g during an event of ML 3.4 in January 2018. A brief history of the earthquakes in the region as well as of the social and political developments afterwards can be found in (Smyrou and Bal 2019), while a more detailed overview is given by (van den Beukel and van Geuns 2019).

Despite the rather small magnitude of these earthquakes, the weak soil characteristics (see Appendix 1), the ground water table very close to the surface, as well as the non-seismic design and construction methods, render the building stock vulnerable. More than 80% of the buildings in the region are unreinforced masonry, 2/3 of which are built by using cavity walls (i.e. two-leaf slender masonry walls with 7-10 cm air gap in between). Although most structures sit on piles or deep foundations, which is not always the case for historical buildings either because the piles were not placed in the first place or have deteriorated over time.

Due to the fact that the earthquakes are of small magnitude, their manifestation is not easily traceable neither by eye nor by sensitive equipment. Even if some movement, which

may be the cause of the damage, is detected, the same amount of movement could also be caused by a number of other factors, such as subsidence, thermal effects etc.

Although it is often claimed, but not supported by evidence, that the earthquakes in Groningen are *"different"*, induced earthquakes are similar to small-magnitude shallow earthquakes in several aspects relevant to structural response (Bal 2018; Bal, Smyrou, and Bulder 2019). The perception of liability, however, is substantially different because the induced earthquakes are caused by third parties and the handling of all consequences is expected to be undertaken by the licensee companies and/or government. In combination with the small magnitude of the earthquakes, this perception does also have a direct impact on the monitoring activities. Vast majority of the sensors and monitoring networks in the Groningen gas field, for example, have been directly or indirectly financed by the licensee company, NAM.

3. Case study structure: Fraeylemaborg in Slochteren

Fraeylemaborg is a noble house built inside a manmade lake in Slochteren, south of Groningen, Netherlands. It is located in an estate of 0.23 km². The house dates back to the 14th century and reached its current form at the end of the 18th century. The structure was built in the 14th century as a house, a defensive dwelling, and grew into an impressive residence by an influential resident. After 1670 the two wings were added giving its U-shaped shape (Figure 1). Following change of owners and a major restoration in 1973, Fraeylemaborg became a museum.
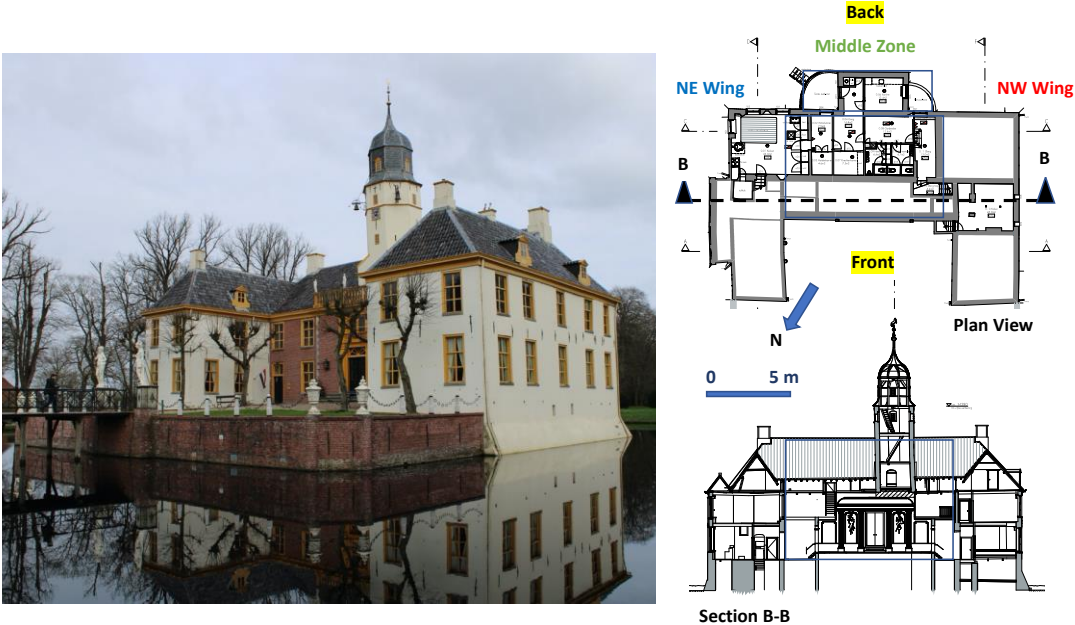

Figure 1. Photograph of Fraeylemaborg (looking from West towards East), plan view and section.

The structure is surrounded by a manmade lake with a water depth of approximately 1.5 m. The main structure has a U-shaped plan consisting of a partial basement, two floors, roof attic and a clock tower (Figure 1). The construction material of the load bearing walls is clay brick with additions of stones in the corners, and metal ties and timber elements in the roof.

The brick-walls are solid and are of varying thickness (40 to 80 cm) in different parts of the structure and the bricks are laid in English bond pattern. Six bricks, retrieved during the previous restoration works, were subjected to compression tests. Their compressive strength was 0.25 MPa in average (standard deviation 0.052 MPa) (Dais et al. 2019), a value considerably lower than those obtained from recent experimental studies (Graziotti et al. 2017;

Graziotti, Penna, and Magenes 2019; Messali et al. 2018; Esposito et al. 2019) on clay bricks currently used in the construction in Groningen. These findings highlight the low capacity of the masonry walls of the structure and raise the question of seismic vulnerability.

The timber elements of the floors are poorly connected to each other and thus a diaphragmatic action is not ensured. Numerous steel anchors exist at various locations of the structure (Figure 1) in order to connect the floors to the peripheral walls. The structural elements of the roof are timber beams transferring the loads to the peripheral walls.

The structure went through a serious renovation in 1973, including structural interventions in the retaining walls outside as well as in the floors and connection details inside the building. There is no written report from that period, but photographs of a personal archive have been used to identify the nature of the structural interventions. As shown in Figure 4, bricks from damaged masonry walls were removed and replaced, however the cause of these damages are unknown. The foundations at the perimeter of the building are also made of brick masonry. They were repaired by using new bricks. A reinforced concrete floor was added above the main entrance, right below the tower. Steel profiles were added at the base of the tower to stabilize it. Finally, all masonry retaining walls were repaired, missing parts were added, and new steel anchors were placed behind the walls.

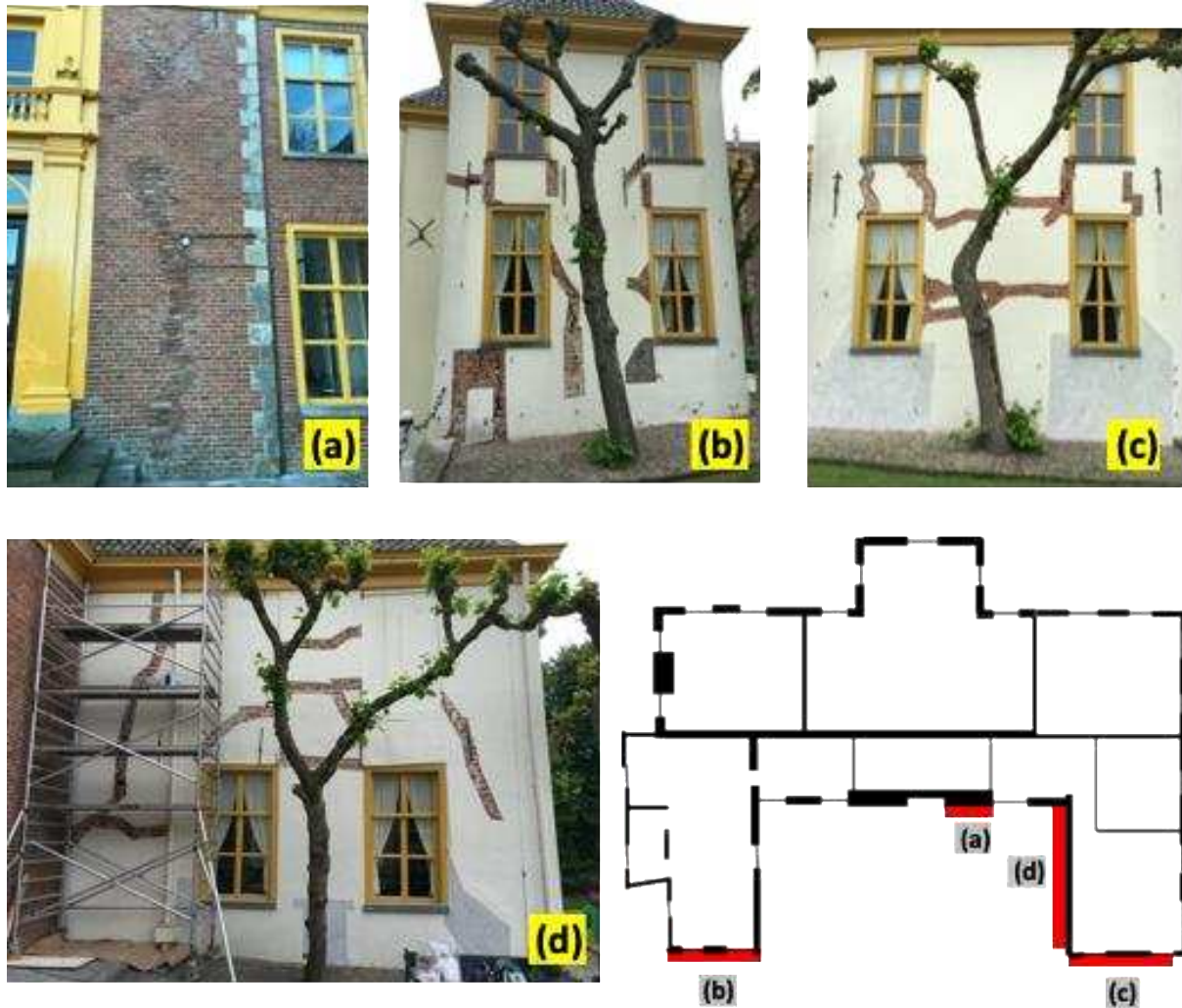Figure 2. Construction phases of the building.

Figure 3. Cracks registered during 2015 restoration, and the red lines on the right-corner plan view denote external walls subjected to damage.

The latest major restoration works took place at the end of 2015 and the beginning of 2017, mostly due to the damage caused by the induced earthquakes in the area. It is highlighted that in 2015 the onset of damages on the structure was recorded while before that no damage was observed. The restorations in 2015-2017 included some structural repair, that was mostly removal and replacement of bricks from the cracked parts of the load bearing walls. These parts were plastered afterwards.
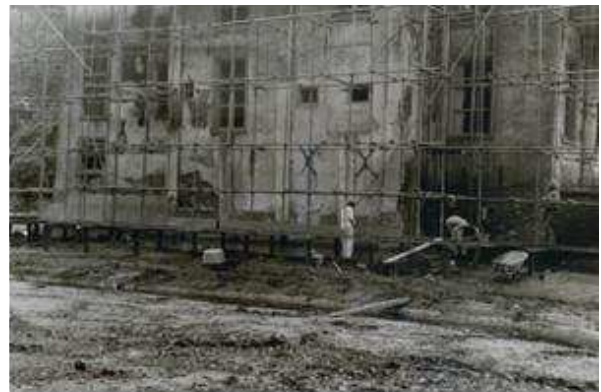
Figure 4. Photos from the restoration Works in 1973, a) a general view from the building under restoration, b) works at foundations along the perimeter, c) mason works on the brick walls, and d) works on the walls and the foundations.

There have been 24 earthquakes above magnitude ML 2.0 since 2012, in epicentral distances 3 to 23 km from the structure. Structural damage and cracks were observed in an increasing pace between 2014 and 2015. The 2015 restoration included interventions on the front façade of the structure where extensive cracks had been formed (Figure 2), while the cracks on the internal walls of the structure were repaired during the 2017 restoration. These cracks were mostly vertical and partly horizontal and diagonal, concentrated on the Northwest (NW) wing as well as on the front façade of the middle zone (see Figure 1) of the structure. The cracks were as wide as a couple of millimetres in some regions. The plaster was removed and the damaged bricks were replaced during the 2015 restoration.

Although the increased seismic activity went hand in hand with increased number of cracks, the shape and location of latter did not resemble earthquake-related cracks. most of them were in vertical direction, with a larger width close to the base and smaller widths in higher elevation, while diagonal X-shaped cracks, the standard sign of in-plane masonry response to lateral earthquake loading, were not observed in the structure. The existing cracks reminded more cracks caused by soil movements rather than by seismic load. After the end of restoration the manifestation of new cracks in the summer of 2018 in the most problematic part of the structure, i.e. the façades of the NW wing (Figure 3), was a puzzlement given the relative limited seismic activity in the respective period. However, after monitoring results have been combined together with finite element analyses and observations in the field, it was possible to reach a plausible explanation for the old (prior to 2015 and in 2015) and the new (summer 2018) damage in the building, as discussed further in this paper.
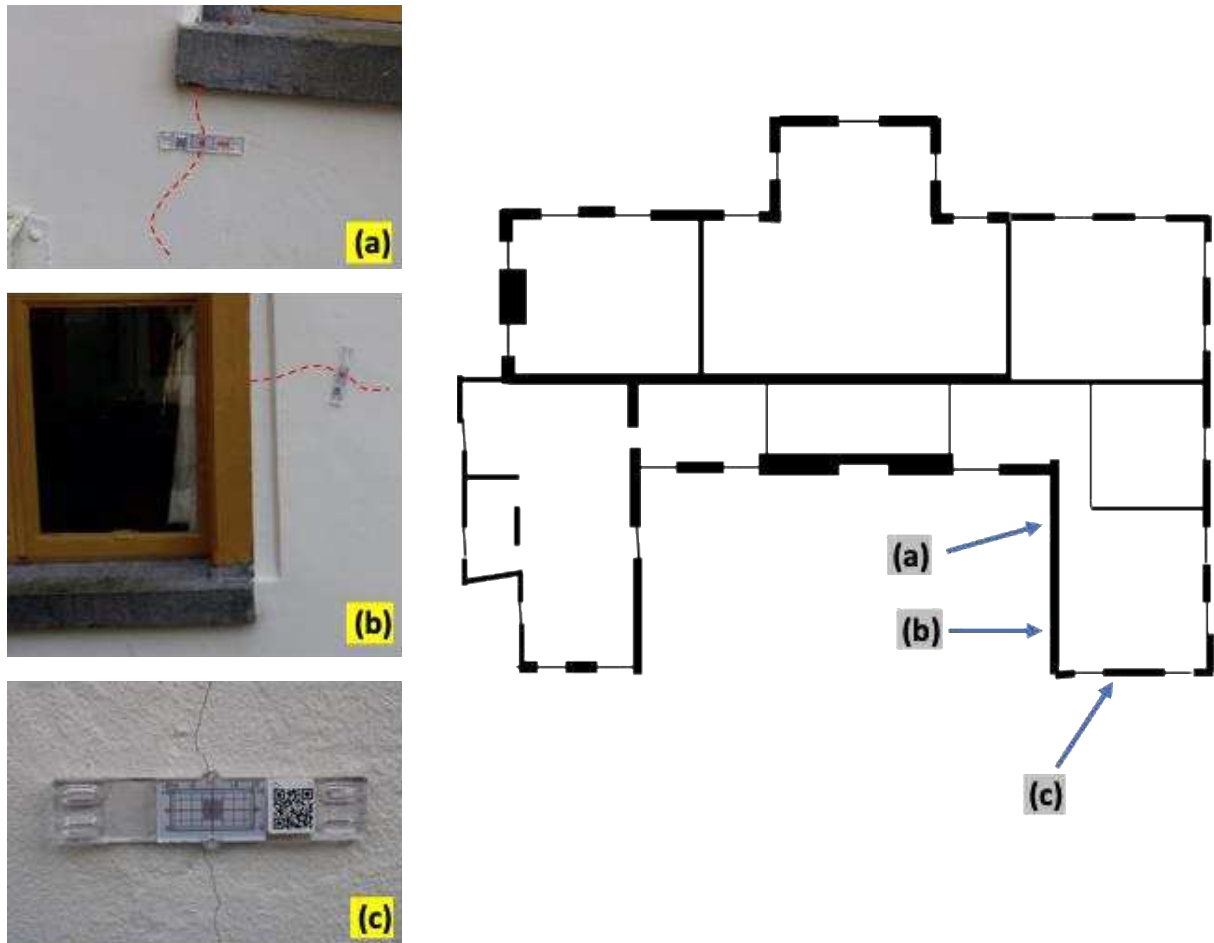
Figure 5. Minor cracks appeared in August 2018 (left) and their locations on the plan view (right).

Fraeylemaborg is being monitored by a tiltmeter at the base since mid-2014, with five 3-axes accelerometers since March 2018, and by analog crack-rulers since March 2019. Ground water data is available starting from mid-2015 while meteorological data is available for more than 10 years. Supplementary to the monitoring activities at Fraeylemaborg (see section 4 for details), soil investigations were also conducted (see Appendix 1). Eight boreholes were drilled around the structure, right outside of the structure and inside the manmade lake after it was drained (Fugro 2018). The boreholes were opened up to 32 m depth at 6 locations and up to 12 m depth at two locations. The upper layers (the first 2-6 m) consist of multiple layers of clay, silty loam, impermeable pot clay ("potklei" in Dutch) and sand, while a uniform sand layer exists after 6-8 m depth. Most of the cone penetration test (CPT) values are below 2 MPa and partly below 4 MPa in the first 5 m. During the soil investigations, the foundation were inspected measuring its dimensions and depth but no information was collected about the existence or condition of any piles.

4. Structural Health Monitoring at Fraeylemaborg and Recent Findings

Structural health monitoring scheme applied at Fraeylemaborg comprises various information channels, i.e. accelerometers, a tiltmeter, analogue crack rulers, meteorological data as well as ground water level measurements. The simultaneous use of multiple channels of information is necessitated by the nature of the induced earthquakes as explained so that reliable conclusions are drawn. The methodology followed is often based on excluding some

of the possible causes and focusing on the most plausible scenarios with the help of multiple sensing data.

The distribution and mounting of accelerometers and the tiltmeter can be seen in Figure 6. The accelerometers used in the seismic SHM system are force-balance type with ultra-low noise levels of 130 ng/Hz0.5. The bandwidth of the sensors is 0.1-120Hz, with a range of +-2 g. More information can be found in the technical sheets of the producer (1). The analogue sensors are connected to a 16-channel digitizer. The data are collected into a computer on site and continuously mirrored in a network mapped hard-drive on a virtual machine. Some example data from a recent ML 3.2 earthquake in May 2019 (Bal and Smyrou 2019a) and the accelerometer and tiltmeter data from 2018 August (Bal and Smyrou 2019b) are digitally available.

Although electronic displacement sensors (potentiometers) were designed for monitoring existing or potential cracks, their installation was avoided due to aesthetic concerns. Instead, crack rulers (see Figure 3c for a clear close-up photo) were placed in January 2019 and monitoring takes place by regularly photographing these crack rulers since then. No movement has been detected since January 2019.

There is a meteorological station in Slochteren the data of which are available online by KNMI. The station data consist of temperature, humidity and rain rate. The station is in less than a kilometre distance from the site.

The ground water level is very well monitored in the region due to significance for the agricultural activities. There are several monitoring wells around the site, but the one that is 600m south of the site, was particularly useful. The level of the ground water is being monitored since April 2015 in this well with 2 hours intervals.

The tiltmeter is an accelerometer-based sensor that detects the inclination of the two perpendicular axes in respect to the vertical axis, by making use of the gravitational acceleration in the vertical direction. The tiltmeter at the basement records in high and low sampling rates. The high sampling rate is 0.01 sec (100 Hz) while the low sampling rate is 15 sec. More data on the technical specifications of the tiltmeter can be found on the technical documentation of the producer (StabiAlert 2019).

---

[1] See product technical specifications at: http://www.teknikdestek.com.tr/tr/urun/13/sensebox702x-703x-?category_id=5
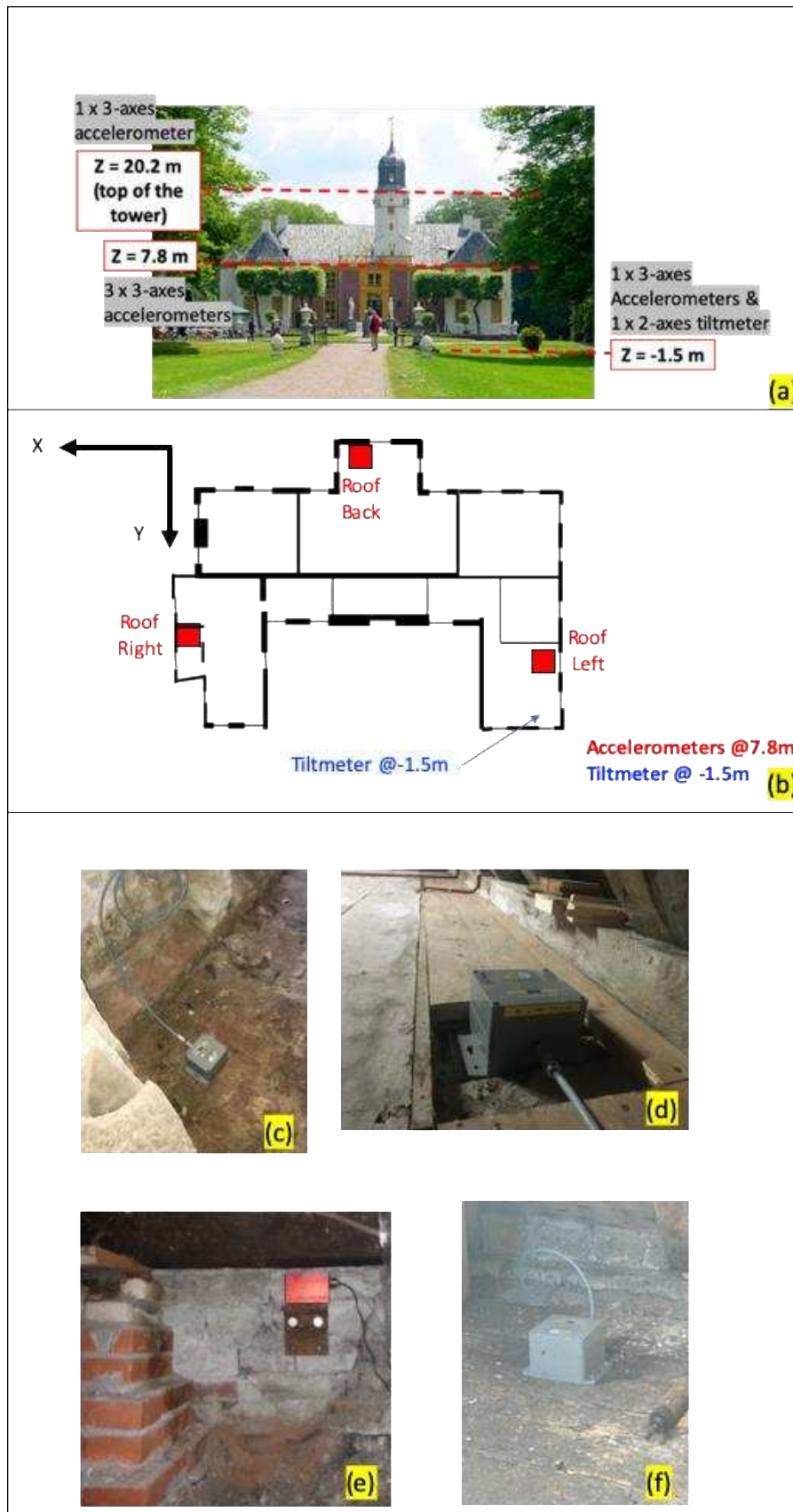
Figure 6. a) elevation of the sensor locations, b) sign convention for the accelerometers and the tiltmeter sensor, c) accelerometer at the basement, d) accelerometer on top of the bearing walls at 7.8m elevation, e) tiltmeter at the basement, and f) accelerometer on the tower floor.

The tiltmeter data since 2014 are given in Figure 7. It should be noted that there was a local repair work in January 2015 and in December 2015 that has shifted the tilt values around both axes. The data jumps around the restoration periods are because of this. In overall, it is evident since the beginning of the monitoring (sometime mid-2014) until the end of the structural restoration and repair (beginning of 2016) that the tilt values systematically increased with the exception of the major structural restoration period that took place right after the Hellum Earthquake of ML 3.1 that occurred just 3 km from the structure. Furthermore, the significant earthquakes (magnitude above 3) recorded during the monitoring period do not present evident effects on the overall plot, however, this may be because the changes in tilt during or after these earthquakes are not big enough and remain concealed by the temporal changes and noise of the tilt measurements. Thus, as explained in detail later, the evaluation of the structural response to each event needs to be done individually. Finally, it is also observed (Figure 7) that the tilt around Y axis is stabilized around a virtual baseline after the restoration and repair works, as only fluctuations for the seasonal changes can be observed after that date. On the contrary, the tilt around X axis exhibits an increasing trend since the end of the restoration and repair works.
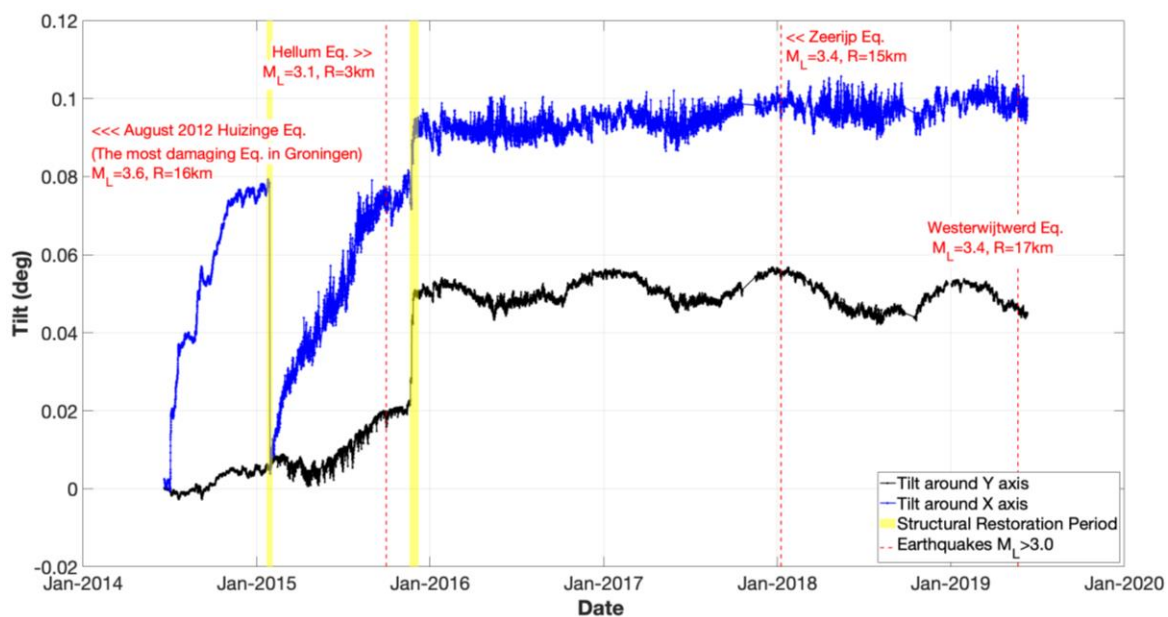

Figure 7. Tiltmeter measurements since 2014, together with significant earthquakes and restoration periods.

Although an earthquake event usually precedes the appearance or deterioration of cracks, it is difficult to establish such an association from the overall plot of tilts. However, focusing on event-based results, better explanations can be obtained that highlight the difference in monitoring when small induced earthquakes are concerned. Two earthquakes were selected for a closer look: the 8th of August 2018 Appingedam earthquake with magnitude ML 1.9 and an epicentral distance of 12 km from the site in the Northeast of the Groningen gas field, and the 22nd of May 2019 Westerwijtwerd earthquake of ML 3.4 in an epicentral distance of 16 km from the site in the Northwest of the gas field. After the former, some damage was reported (see Figure 3), while the day of the latter, as well as a week before and a week after, the crack rulers were photographed, with no movement or additional crack being detected. Considering that the purpose of this paper is to discuss the different methodologies needed in seismic SHM

in case of induced earthquakes, these two earthquake events constitute a good comparative example as explained below in detail.

The Appingedam earthquake (ML 1.9) was recorded by the accelerometers in the building (the full dataset is available online in open source by (Bal and Smyrou 2019b).The time-histories at the basement, at the roof level on the two wings of the structure as well as at the tower are given in Figure 8. The presented time-histories are baseline corrected and bandpass Butterworth filtered between 0.1-20 Hz. The motion was detected by the sensors although the maximum accelerations do not exceed 1 cm/sec^2 (0.001 g). The tower amplified the input motion approximately 3 times, while the structure itself amplified it 2 times, both still remaining well below the horizontal acceleration levels that would normally cause any cracks.
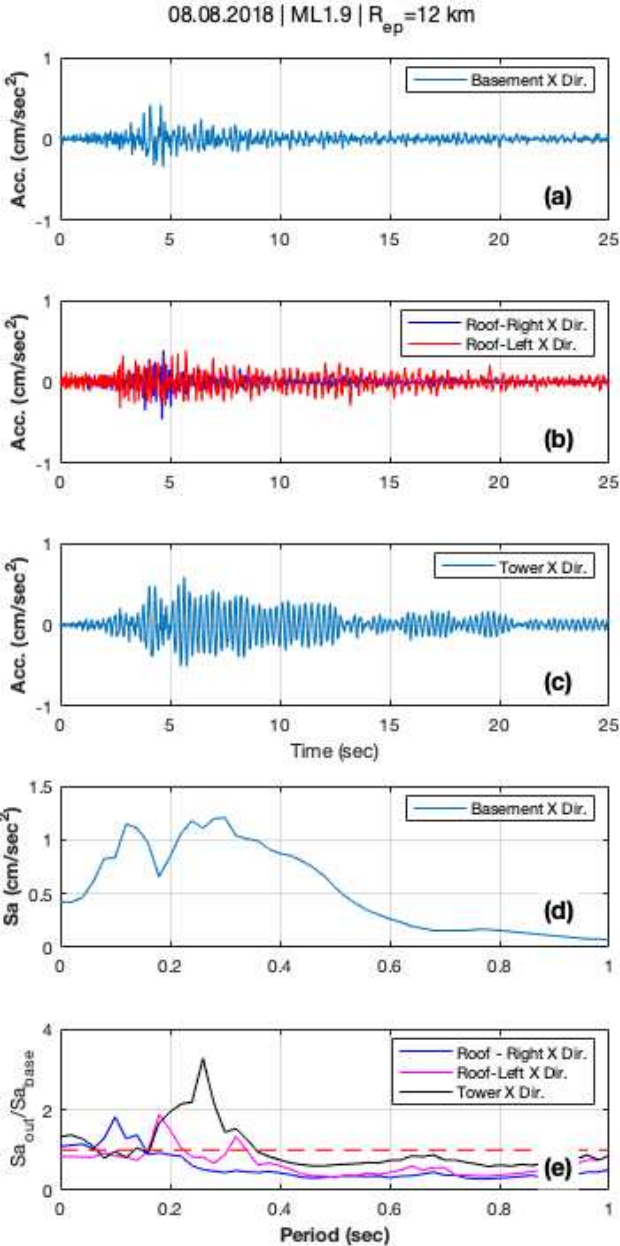

Figure 8. For the 8th of August 2018 Appingedam Earthquake of ML 1.9 in epicentral distance of 12 km are presented: acceleration time-histories (Acc.) in the X direction for the sensors at (a) the basement level, (b) the roof level (right and left side of the structure, shown in Figure 4b), and (c) the tower, (d) 5% damped spectral acceleration (Sa) as obtained from the sensor at the basement in the X direction, and (e) transfer functions (spectral acceleration on the structure (Sa$_{out}$) divided by the spectral acceleration at the base (Sa$_{base}$)).

During the seismic excitation the fluctuation of tilt recorded was rather insignificant. Thus, only examining real-time tilt data would not offer an insight into the degree of damage that actually led to the formation of new cracks. In order to better understand the cause of damage, low sampling rate tiltmeter data have also been examined (Figure 9). For the last 15 days before the earthquake the daily temperature cycles oscillate on average around a baseline but the motion builds up in a way in the three days following the earthquake. From the 4th to 15th day after the earthquake tilt values in both axes increase significantly jumping to a new baseline. Furthermore, the range of angles in daily temperature changes also decreases causing the tilt values to fluctuate in a narrower band. A new baseline of tilt values indirectly signifies a certain level of plastic deformation, indicating that damage took place.

It is naturally expected that the tilt values are highly influenced by the temperature changes. In order to decouple the temperature effects from the measurements, plots in Figure 10 were prepared where the 30-day period (15 days before and 15 days after the earthquake) have been plotted against the measured ambient temperature. Furthermore, in order to understand the progress of the tilt, the exact same 30-day periods are also plotted for one and two years before (2017 and 2016 respectively) for the same period of the year. These data are used to understand the relevance of the observed damages with the Appingedam Earthquake of ML 1.9. The first and striking observation is that the temperatures in 2018 were much higher than the prior two years, which led to a different correlation between the ambient temperature and the tilt values in the range of 25 °C to 30 °C. Furthermore, it was shown that the relationship between the tilt values and the temperature is within an expected range 15 days before the earthquake (green lines) and 3 days following the earthquake (orange lines), while 4th to 15th days after the earthquake a different relationship is observed (red lines), where the tilt values increase independent of the temperature values. In brief, it is concluded that the change of baseline in the tilt values is not related to the ambient temperature.
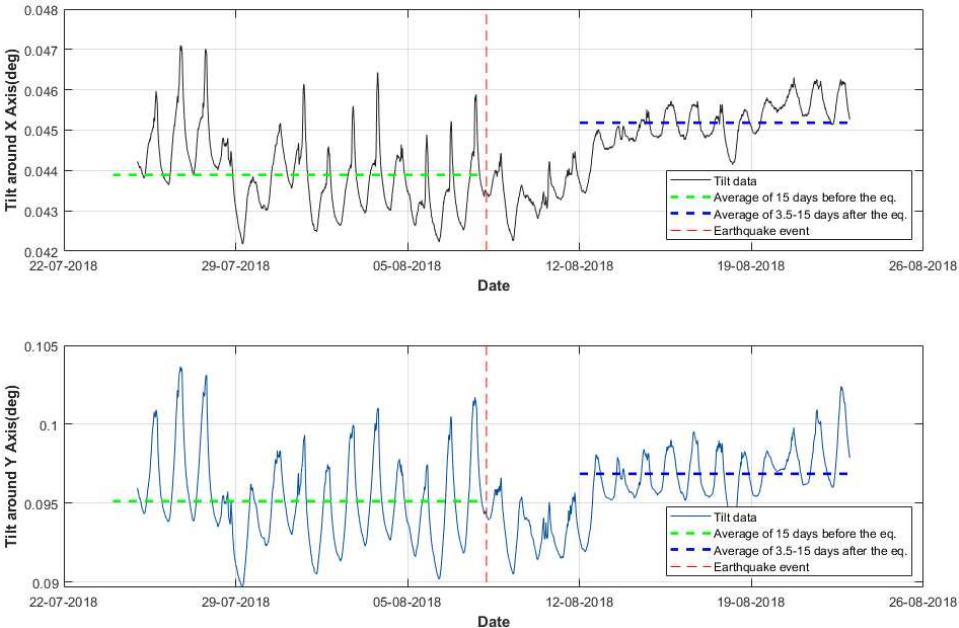

Figure 9. Low sampling rate tiltmeter data 15 days before and 15 days after the earthquake of 08.08.2018 Appingedam (ML 1.9).
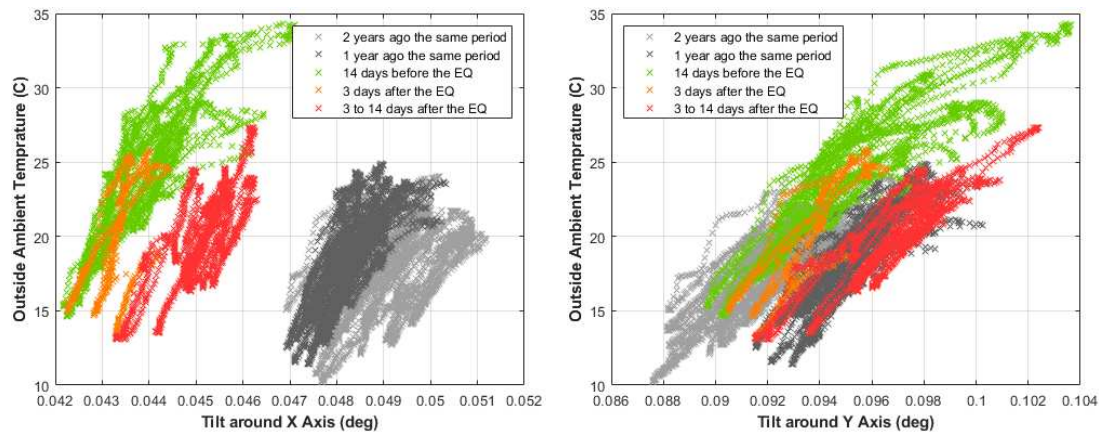
Figure 10. Tilt angles recorded +-15 days from the earthquake and last two years before.

The tiltmeter data, in combination with the accelerometers data from 8th of August 2018 event, indicate that the foundation of the NW wing and the soil beneath have played an important role in the cracks that appeared in August 2018. It is difficult to explain the exact contribution of soil-related parameters since fundamental data, such as the potential existence and the situation of piles, are unknown. Speculation about possible explanations regarding the soil effects are provided below.

As mentioned before, soil properties of the site were determined by using 8 boreholes and CPT tests (see Appendix 1). The two boreholes right next to the NW wing, where the damage concentration occurred, revealed a different soil profile in the first 6m from that in the Northeast (NE) side. NE side is mostly sand, while NW side consists mostly of loam, silt and clay (pot clay or "potklei" in Dutch) layers dominating in the first 2-6 meters.

The shrinking or/and the expansive behaviour of the clay layers may be responsible for the structural cracks considering that clay soils can be responsive to moist cycles. Certain clay types are expansive soils, and early studies have identified potential problems for the foundations sitting on such soils (Popescu 1986; Nelson and Miller 1992). When shrinking or swelling, certain clay soils apply a level of pressure to the environment, including structural foundations (Basma, Al-Homoud, and Husein 1995). Specific clay types can also crack due to lack of water, up to some meters of depth (Morris, Graham, and Williams 1992), decreasing the bearing capacity substantially. There are several regions with similar soils in the Netherlands (Bouma 1980).

Part of the NW wing of the structure is sitting on pot clay layers of several meters thick, a highly impermeable and stiff clay material. Swelling tests conducted on pot clay layers in the region[2] show that expansion can be limited to less than 1% in volume but considerable shrinking is possible when the layers dry out completely. Due to the high impermeability water is hindered and thus the expansion is limited. Shrinking, however, can still be an issue for pot clay.

Another possible explanation may be related to the piles under the foundation. Due to the weak soil conditions in the region, it is almost impossible to construct any structure without piles. It is thus expected that Fraeylemaborg, being a relatively heavy structure as compared to the modern ones, would also be sitting on some sort of pile grid. Because of the historical identity of the building, access to certain parts is not allowed, thus the existence of the piles is not confirmed. Nevertheless, the common construction practice in the region dictates that some wooden piles must exist under the foundations. If this is the case, especially the old wooden piles need to be under water for protection from deterioration. It is known that draught causes adverse effects on wooden piles in historical buildings.

---

[2] Personnal communication with Onno Dijkstra from Fugro in Groningen.

The scenarios for relating the soil response to structural cracks given above are based on water conditions. One may consider that the structure is surrounded by a manmade lake thus the soil layers are always under water, however this is not granted since the dominating layers are highly impermeable clays and thus the soil layers right beneath the foundations may still be dry in case of draught.

The ground water movement in the same days was also investigated. The rain rate is plotted in Figure 11 together with the ground water measurements, in order to decouple possible ground water raise due to the earthquake action. The ground water is monitored in the monitoring well with approximately 4 m total depth. Due to the monitoring setup, the sensors used and the sampling rate (2 hours), the monitoring data can provide only slow movements of ground water and not the changes during the seconds of the earthquake motion.

Figure 9 reveals a very dry period from mid-March to mid-August in 2018, reported as a disastrous period for the farmers in the region due to the extremely dry soil. It was also witnessed in soil drilling works that the clay layers were hard and dry due to lack of rain for a very long period. As seen in Figure 11 the start of the rainy period coincides with the earthquake (in fact, a couple of days later). When other rainy periods in the data are examined, tiltmeter data are found mostly insensitive to the rain. Furthermore, the out-of-the-ordinary movement (i.e. change in tilt baseline) in the tiltmeter data starts right after the earthquake, proving that the movement is related to the earthquake motion too.
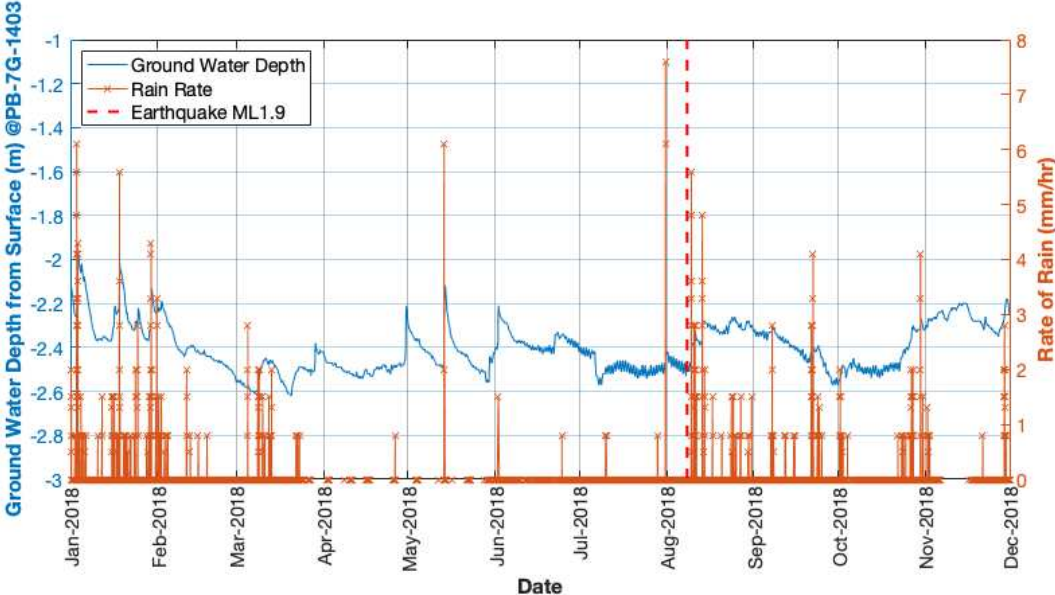

Figure 11. Ground water depth from the surface and the rate of rain in 2018 in the monitoring well 600 m south of the site.

Based on all available data, the most plausible scenario for explaining the damages in August 2018 is studied. The structure has light floors and a light timber roof, while the bearing walls are relatively thick. In-plane cracks would not be expected in this structure during such small earthquakes. One possible explanation is that the soil parameters such as shrinking of water-sensitive soil layers and/or response of piles, in combination with a small distant earthquake, caused settlements and/or increased the stress levels on foundations. In other words, the soil effects might have superimposed with the earthquake motion and caused the small cracks. Nonlinear finite element analyses have also been run for supporting this scenario, as presented further.

If the monitoring results constituted merely by acceleration measurements, one could argue that the structure should have had much more cracks after the 22nd of May 2019 earthquake of ML 3.4 since the accelerations at the base, on the structure and at the tower were much higher than the respective of the event in the 8th of August 2018 (Bal and Smyrou

2019a). Note that the horizontal PGA at the basement was 0.004 g and the maximum absolute horizontal acceleration at the tower was recorded as 0.03 g. Although still very small, these accelerations are larger, more than an order of magnitude, as compared to the acceleration levels of the August 2018 event (Figure 12). A detailed check on the photographs of the crack rulers showed that no significant movement took place during the May 2019 earthquake. When the tilt data of 15 days before and 15 days after were examined, no change of tilt baseline or any other out-of-the-ordinary movement was observed. Had the seismic SHM system relied only on the accelerometer data, the fact that the August 2018 earthquake caused damages, while the stronger (in terms of acceleration) May 2019 earthquake caused no damage, would be inexplicable.

In order to better understand the damage mechanism of the structure, a non-linear 3D finite element model was constructed without considering the soil layers. In the numerical model the structural elements are taken into consideration as the masonry walls and the timber slabs. The timber slab elements are characterized by the lack of proper connections to each other and to the walls, and thus there is absence of diaphragmatic action. This behaviour was incorporated in the model by accounting for rather low stiffness for the slabs. Given the lack of any experimental data for the materials found in the structure, the elastic properties of the model calibrated against ambient vibration tests that took place on site. More details on the site tests and on the nonlinear material properties can be found in Dais et al. (2019). The model was able to accurately reproduce the experimentally obtained mode shapes of the structure both global and local.

Given the fact that no damage has been observed in the timber elements, they were modelled as linear elastic. For the masonry walls, nonlinear elements were utilized based on the Concrete Damage Plasticity constitutive law, already implemented in ABAQUS (ABAQUS 2013). This is a common numerical approach that has been used extensively to simulate historical URM structures (Castellazzi et al. 2018; Sarhosis et al. 2018; Valente and Milani 2019). This model is able to reproduce the different strength in tension and compression that characterizes masonry elements.

The nonlinear numerical model was subjected to different scenarios to see if a correlation can be established between the analytical findings and the past damage. As explained in (Dais et al. 2019), there are findings (i.e. crack patterns, concentration of damage) in the structure that support the occurrence of a soil settlement in the NW wing, thus a settlement was applied in that wing analytically. In particular, a 0 to 0.5 cm vertical settlement is applied on the NW wing (i.e. 0.5 cm at the edge, 0 cm at the connection with the main zone) and the response of the structure is shown in terms of tensile maximum principal stresses (Figure 13). In case of the scenario of only-settlement, although some of the cracks prior to the renovation and repair in 2015 (Figure 2) were captured, the results were not satisfactory in overall. Match between the damage distribution and the observed damages was not achieved. When an earthquake load is applied in conjunction with the settlement, the location of the cracks in the NW wing and at the front façade of the main zone were captured successfully (see the comparison in Figure 13). The earthquake load is applied as incremental lateral equivalent static force proportionally to the mass and from 0 to 0.08g. The earthquake load is applied in the short direction of the structure because this was the dominant direction of the 2015 Hellum Earthquake of ML 3.1 (i.e. the direction perpendicular to the travel path). Hellum Earthquake was reported as the reason of the damages in the structure in 2015 and the crack photos presented in Figure 2 belong to a period right after that earthquake.

The point of this numerical exercise is to show distribution of cracks derived after the combination of two actions. In more detail, when settlements are applied, concertation of damage is observed at the wall shown in Figure 2d and beneath the tower. After the superposition of seismic load, further damage appears at the walls as also shown in Figure 2a, b and c.
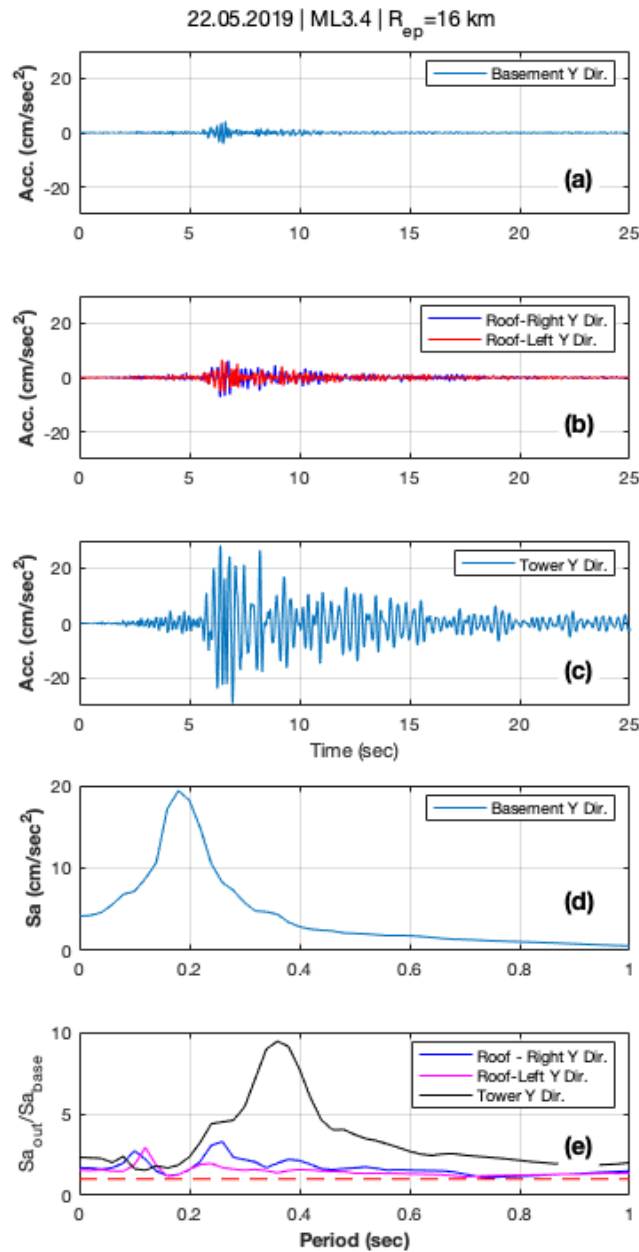
Figure 12. For the 22nd of May 2019 Westerwijtwerd Earthquake of ML 3.4 in epicentral distance of 16 km are presented: acceleration time-histories (Acc.) in the Y direction for the sensors at (a) the basement level, (b) the roof level (right and left side of the structure, shown in Figure 4b), and (c) the tower, (d) 5% damped spectral acceleration (Sa) as obtained from the sensor at the basement in the Y direction, and (e) transfer functions (spectral acceleration on the structure (Sa_{out}) divided by the spectral acceleration at the base (Sa_{base})).
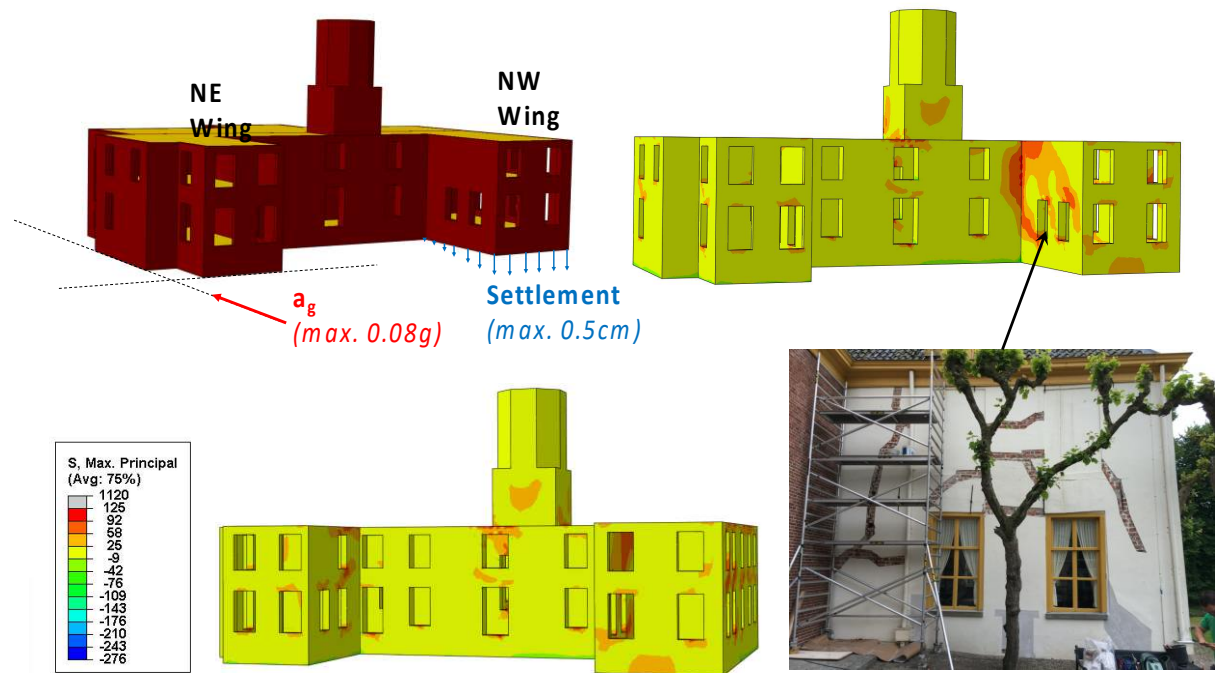
Figure 13. Distribution of maximum principal stresses from the nonlinear static analyses in the scenario of 0.5cm maximum vertical settlement at the NW wing superposed with lateral earthquake equivalent static load of 0.08g and comparison with the observed damages after 2015 Hellum Earthquake.

5.   Conclusions

The increasing number of deep underground energy exploitation projects around the world is associated with induced earthquakes, which are usually small in magnitude and recursive. In most cases, they occur in areas without prior seismic activity, meaning that the building stock is inherently vulnerable to seismic loads.

Due to their effects on the built environment, induced earthquakes in the Groningen Gas Field in the north Netherlands have triggered intense research on the response of unreinforced masonry to induced earthquakes. An extended seismic monitoring network has also been established. Although there are more than 2,000 historically registered buildings in the region, only a single building is being monitored by using standard seismic SHM techniques, that is the topic of this paper. The monitoring results of that historical building, Fraeylemaborg in Slochteren, are presented here to create a basis of discussion on what would be the main differences when monitoring historical buildings in case of induced earthquakes.

Two earthquakes and the relevant monitoring data are used to better explain the goals of this paper. First, a small and distant earthquake with reported slight damages has been investigated by using accelerometer, tiltmeter, soil investigation, ground water monitoring and meteorological data. Second, a recent earthquake with much higher recorded accelerations in the structure, but without any reported damage has been studied. The seemingly controversial nature of the damages of these two cases has been discussed by using supporting monitoring data and finite element modelling. Although conclusions on causes of damages cannot be of absolute certainty, as usually is the case in induced seismicity, plausible scenarios have been proposed and discussed in detail. In this way, it was shown that measurements that are based on a single source of sensors, such as only tiltmeters or only accelerometers, would not be enough to provide reasonable explanations. Furthermore, it was also shown that the meteorological data play a critical role in developing damage scenarios in case of induced seismicity. From the above it is evident that the potential to employ continuous, real-time and automatic structural health monitoring system is beneficial for the detection of causes of

damage but also for the early detection of a potentially dangerous situation for the structure and its occupants.

In brief, Fraeylemaborg is used here as an exemplary case that shows that the effects of induced small-magnitude earthquakes may not be immediately evident or may be overshadowed or concealed with other causes. Furthermore, it was also shown here that in case of induced small earthquakes, seemingly misleading monitoring results may have meaning, thus even the data that seem irrelevant should be examined with an open-minded approach. It was shown in this work that, in case of damage to historical masonry due to small recursive earthquakes, combination of techniques and tailor-made solutions are needed.

As a side note, and relevant to the climate adaptation problems in the world in recent years, it is shown here that the changing climate ultimately can play a role in structural damage, even to the structures that have survived hundreds of years.

Based on all available data, the damages at Fraeylemaborg are studied. It was concluded that the in-plane cracks would not be expected in this structure during such small earthquakes. One explanation could be that the soil parameters, such as shrinking of water-sensitive soil layers and/or response of piles, in combination with a small distant earthquake, caused settlements and/or increased the stress levels on foundations. The soil effects might have superimposed with the earthquake effects causing small cracks.

In the future, the work of the authors in Fraeylemaborg will continue to better understand the nature of the damages. As part of that effort, a nonlinear FE model with a properly modelled soil box is prepared and will be run to investigate further the soil-structure interaction phenomena associated with induced seismicity events. Furthermore, in order to better capture the ground water movements during the earthquake, two monitoring wells are planned to be installed exactly on the site, right outside of the artificial lake. These monitoring spots will provide pore pressure data and ground water height data with 100 Hz sampling.

Acknowledgements

References

ABAQUS. 2013. Analysis User's Manual, 6.13-3. RI, USA: Dassault Systems Providence.

Bal, İ. E. 2018. Myths and Fallacies in the Groningen Earthquake Problem. Groningen: Hanze University of Applied Sciences, Groningen - Research Centre for Built Environment – NoorderRuimte.

Bal, İ. E., and E. Smyrou. 2019a. Unprocessed Accelerometer Data from Fraeylemaborg, Slochteren, during 22.05.2019 Westerwijtwerd Earthquake of ML3.4. doi:10.4121/uuid:46b9b3c9-5d5f-468c-aab8-980260c7a0d2.

Bal, İ. E., and E. Smyrou. 2019b. Unprocessed Accelerometer and Tiltmeter Data from Fraeylemaborg, Slochteren, during 08.08.2018 Appingedam Earthquake of ML1.9. doi:10.4121/uuid:fbd8e340-1943-4d13-ac75-0bc038690f43.

Bal, İ. E., E. Smyrou, and E. Bulder. 2019. Liability and Damage Claim Issues in Induced Earthquakes: Case of Groningen. In SECED 2019 Conference. Greenwich, UK.

Basma, A. A., A. S. Al-Homoud, and A. Husein. 1995. Laboratory Assessment of Swelling Pressure of Expansive Soils. Applied Clay Science 9 (5): 355–368. doi:10.1016/0169-1317(94)00032-L.

Bouma, J. 1980. Field Measurement of Soil Hydraulic Properties Characterizing Water Movement through Swelling Clay Soils. Journal of Hydrology 45 (1–2): 149–158. doi:10.1016/0022-1694(80)90011-6.

Çaktı, E., and E. Şafak. 2019. Structural Health Monitoring: Lessons Learned. In Seismic Isolation, Structural Health Monitoring, and Performance Based Seismic Design in Earthquake Engineering, edited by A. A. Kasimzade, E. Şafak, C. E. Ventura, F. Naeim, and Y. Mukai, 145–164. Cham: Springer International Publishing. doi:10.1007/978-3-319-93157-9_5.

Castellazzi, G., A. M. D'Altri, S. de Miranda, A. Chiozzi, and A. Tralli. 2018. Numerical Insights on the Seismic Behavior of a Non-Isolated Historical Masonry Tower. Bulletin of Earthquake Engineering 16 (2): 933–961. doi:10.1007/s10518-017-0231-6.

Ceravolo, R., A. De Marinis, M. L. Pecorelli, and L. Zanotti Fragonara. 2017. Monitoring of Masonry Historical Constructions: 10 Years of Static Monitoring of the World's Largest Oval Dome. Structural Control and Health Monitoring 24 (10): e1988. doi:10.1002/stc.1988.

Cigada, A., L. Corradi Dell'Acqua, B. Mörlin Visconti Castiglione, M. Scaccabarozzi, M. Vanali, and E. Zappa. 2017. Structural Health Monitoring of an Historical Building: The Main Spire of the Duomo Di Milano. International Journal of Architectural Heritage 11 (4): 501–518. doi:10.1080/15583058.2016.1263691.

Coïsson, E., and C. Blasi. 2015. Monitoring the French Panthéon: From Rondelet's Historical Surveys to the Modern Automatic System. International Journal of Architectural Heritage 9 (1): 48–57. doi:10.1080/15583058.2013.793437.

Crowley, H., R. Pinho, B. Polidoro, and J. van Elk. 2017. Developing Fragility and Consequence Models for Buildings in the Groningen Field. Netherlands Journal of Geosciences 96 (5): s247–s257. doi:10.1017/njg.2017.36.

Dais, D., E. Smyrou, İ. E. Bal, and J. Pama. 2019. Monitoring, Assessment and Diagnosis of Fraeylemaborg in Groningen, Netherlands. In Aguilar R., Torrealva D., Moreira S., Pando M.A., Ramos L.F. (Eds) Structural Analysis of Historical Constructions. RILEM Bookseries, Vol 18. Springer, Cham, 2188–2196. doi:10.1007/978-3-319-99441-3_235.

Erdik, M. 2018. Seismic Isolation, Structural Health Monitoring, and Performance Based Seismic Design in Earthquake Engineering. Seismic Isolation, Structural Health Monitoring, and Performance Based Seismic Design in Earthquake Engineering. Springer International Publishing. doi:10.1007/978-3-319-93157-9.

Esposito, R., F. Messali, G. J. P. Ravenshorst, H. R. Schipper, and J. G. Rots. 2019. Seismic Assessment of a Lab-Tested Two-Storey Unreinforced Masonry Dutch Terraced House. Bulletin of Earthquake Engineering 17 (8): 4601–4623. doi:10.1007/s10518-019-00572-w.

Fugro. 2018. Geotechnisch Onderzoek FRAEYLEMABORG TE SLOCHTEREN. Report No.: 1318-0270-000.

Gonçalves, L. M. S., H. Rodrigues, and F. Gaspar. 2017. Nondestructive Techniques for the Assessment and Preservation of Historic Structures. Edited by L. M. da S. Gonçalves, H. Rodrigues, and F. Gaspar. CRC Press. doi:10.1201/9781315168685.

Graziotti, F., A. Penna, and G. Magenes. 2019. A Comprehensive in Situ and Laboratory Testing Programme Supporting Seismic Risk Analysis of URM Buildings Subjected to Induced Earthquakes. Bulletin of Earthquake Engineering 17 (8): 4575–4599. doi:10.1007/s10518-018-0478-6.

Graziotti, F., U. Tomassetti, S. Kallioras, A. Penna, and G. Magenes. 2017. Shaking Table Test on a Full Scale URM Cavity Wall Building. Bulletin of Earthquake Engineering 15 (12). Springer Netherlands: 5329–5364. doi:10.1007/s10518-017-0185-8.

Kita, A., N. Cavalagli, and F. Ubertini. 2019. Temperature Effects on Static and Dynamic Behavior of Consoli Palace in Gubbio, Italy. Mechanical Systems and Signal Processing 120 (April). Elsevier Ltd: 180–202. doi:10.1016/j.ymssp.2018.10.021.

KNMI. 1993. Netherlands Seismic and Acoustic Network. Royal Netherlands Meteorological Institute (KNMI). Other/Seismic Network. doi:10.21944/e970fd34-23b9-3411-b366-e4f72877d2c5.

Messali, F., R. Esposito, S. Jafari, G. J. P. Ravenshorst, P. A. Korswagen Eguren, and J. G. Rots. 2018. A Multiscale Experimental Characterisation of Dutch Unreinforced Masonry Buildings. In Proceedings of 16th European Confer- Ence on Earthquake Engineering (ECEE).

Morris, P. H., J. Graham, and D. J. Williams. 1992. Cracking in Drying Soils. Canadian Geotechnical Journal 29 (2): 263–277. doi:10.1139/t92-030.

Nelson, J. D., and D. J. Miller. 1992. Expansive Soils – Problems and Practice in Foundation and Pavement Engineering, Wiley Professional Paperback Series, John Wiley & Sons.

Popescu, M. E. 1986. A Comparison between the Behaviour of Swelling and of Collapsing Soils. Engineering Geology 23 (2): 145–163. doi:10.1016/0013-7952(86)90036-0.

Ramos, L. F., L. Marques, P. B. Lourenço, G. De Roeck, A. Campos-Costa, and J. Roque. 2010. Monitoring Historical Masonry Structures with Operational Modal Analysis: Two Case Studies. Mechanical Systems and Signal Processing 24 (5): 1291–1305. doi:10.1016/j.ymssp.2010.01.011.

Rossi, P. P., and C. Rossi. 2015. Monitoring of Two Great Venetian Cathedrals: San Marco and Santa Maria Gloriosa Dei Frari. International Journal of Architectural Heritage 9 (1): 58–81. doi:10.1080/15583058.2013.793435.

Saisi, A., and C. Gentile. 2015. Post-Earthquake Diagnostic Investigation of a Historic Masonry Tower. Journal of Cultural Heritage 16 (4). Elsevier Masson SAS: 602–609. doi:10.1016/j.culher.2014.09.002.

Sarhosis, V., D. Dais, E. Smyrou, and İ. E. Bal. 2019a. Computational Modelling of Damage Accumulation in Unreinforced Masonry Dutch Constructions Subjected to Induced Seismicity. In SECED 2019 Conference. Greenwich, UK.

Sarhosis, V., D. Dais, E. Smyrou, and İ. E. Bal. 2019b. Evaluation of Modelling Strategies for Estimating Cumulative Damage on Groningen Masonry Buildings Due to Recursive Induced Earthquakes. Bulletin of Earthquake Engineering 17 (8): 4689–4710. doi:10.1007/s10518-018-00549-1.

Sarhosis, V., G. Milani, A. Formisano, and F. Fabbrocino. 2018. Evaluation of Different Approaches for the Estimation of the Seismic Vulnerability of Masonry Towers. Bulletin of Earthquake Engineering 16 (3): 1511–1545. doi:10.1007/s10518-017-0258-8.

Smyrou, E., and İ. E. Bal. 2019. Guest Editorial for the Special Issue on Induced Seismicity and Its Effects on Built Environment. Bulletin of Earthquake Engineering 17 (8): 4411–4415. doi:10.1007/s10518-019-00672-7.

StabiAlert. 2019. Structural Health Sensor. Report Available at Https://Www.Stabialert.Nl/Fileadmin/Stabialert2017/Downloads/Specsheet__Safety_from_every_angle_-_Structural_Health_Sensor.Pdf. Accessed 14 Jul 2019.

Valente, M., and G. Milani. 2019. Damage Assessment and Collapse Investigation of Three Historical Masonry Palaces under Seismic Actions. Engineering Failure Analysis 98 (April): 10–37. doi:10.1016/j.engfailanal.2019.01.066.

van den Beukel, J., and L. van Geuns. 2019. Groningen Gas: The Loss of a Social License to Operate. Report for The Hauge Centre for Strategic Studies, HCSS Geo-Economics, The Hauge, Netherlands.

van Elk, J., and D. Doornhof. 2017. Induced Seismicity in Groningen, Assessment of Hazard, Building Damage and Risk, NAM Reports.

van Thienen-Visser, K., and J. N. Breunese. 2015. Induced Seismicity of the Groningen Gas Field: History and Recent Developments. The Leading Edge 34 (6): 664–671. doi:10.1190/tle34060664.1.

Appendix 1 – Representative Soil Data

N

DP2

Sand	*qc=1-2 MPa*
Clay	*qc=1 MPa*
Sand	*qc=2-8 MPa*
Clay	*qc=1 MPa*
Pot Clay	*qc=1 MPa*
Sand	*qc=18-33 MPa*
Clay	*qc=12 MPa*
Sand	*qc=24-32 MPa*
Clay	*qc=10 MPa*

0
-10 m
-20 m
-28 m

DP5

Sand	*qc=1-6MPa*
Clay	*qc=1MPa*
Pot Clay	*qc=1-3MPa*
Clay	*qc=1-3MPa*
Sand	*qc=8-33MPa*

0
-10 m
-20 m
-32 m

DP7

Sand	*qc=1-4 MPa*
Clay	*qc=1-6 MPa*
Pot Clay	*qc=1 MPa*
Clay	*qc=1-2 MPa*
Sand	*qc=10-24 MPa*
Clay	*qc=22-26 MPa*
Sand	*qc=16-22 MPa*
Clay	*qc=8-10 MPa*

0
-10 m
-20 m
-32 m